# Effect of Cation Size and Disorder on the Structure and Properties of the Rare Earth Cobaltates, $Ln_{0.5}A_{0.5}CoO_3$ ($Ln = $ Rare Earth, $A = Sr, Ba$)

P. V. Vanitha, Anthony Arulraj, P. N. Santhosh, and C. N. R. Rao*

*Chemistry and Physics of Materials Unit and CSIR Center of Excellence in Chemistry,*
*Jawaharlal Nehru Center for Advanced Scientific Research, Jakkur P.O.,*
*Bangalore 560 064, India*

*Received May 5, 1999. Revised Manuscript Received March 28, 2000*

The structure of $Ln_{0.5}Sr_{0.5}CoO_3$ is rhombohedral ($R\bar{3}c$) when Ln = La, Pr, or Nd, but orthorhombic ($Pnma$) when Ln = Gd. The $Ln_{0.5}Ba_{0.5}CoO_3$ compounds, except for Ln = La, are orthorhombic ($Pmmm$). The ferromagnetic Curie temperature, $T_C$, of $Ln_{0.5}A_{0.5}CoO_3$ increases with the average size of the A-site cation up to an $\langle r_A\rangle$ of 1.40 Å, and decreases thereafter due to size mismatch. Disorder due to cation-size mismatch has been investigated by studying the properties of two series of cobaltates with fixed $\langle r_A\rangle$ and differing size variance, $\sigma^2$. It is found that $T_C$ decreases linearly with $\sigma^2$, according to the relation, $T_C = T°_C - p\sigma^2$. When $\sigma^2$ is large (>0.012 Å$^2$), the material becomes insulating, providing evidence for a metal−insulator transition caused by cation-size disorder. Thus, $Gd_{0.5}Ba_{0.5}CoO_3$ with a large $\sigma^2$ is a charge-ordered insulator below 340 K. The study demonstrates that the average A-cation radius, as well as the cation-size disorder, affects the magnetic and transport properties of the rare earth cobaltates significantly.

## Introduction

Rare earth cobaltates of the formula $Ln_{0.5}Sr_{0.5}CoO_3$ (Ln = rare earth) are known as metallic ferromagnets and their electrical and magnetic properties have been described adequately in the literature.[1] The ferromagnetic Curie temperature, $T_C$ , in these materials decreases significantly with the decrease in the size of the rare earth ion. The magnetic and electrical properties of the barium-substituted cobaltates of the formula $Ln_{0.5}Ba_{0.5}CoO_3$ are different from those of the strontium analogues. Recent studies show that the barium-substituted cobaltates exhibit a insulator−metal transition when the radius of the rare earth ion is small.[2,3] Thus, $Gd_{0.5}Ba_{0.5}CoO_3$ is a charge-ordered insulator, although there are some differences in the published reports regarding its electrical properties.[2−4] Structures of the $Ln_{0.5}A_{0.5}CoO_3$ (A = Sr, Ba) compounds also vary with Ln and A, although there are conflicting structural assignments in the literature. Thus, $Ln_{0.5}Sr_{0.5}CoO_3$ have generally been considered to be cubic, although the possible orthorhombicity has been indicated recently.[5] In the corresponding Ba compounds, cubic, tetragonal, and orthorhombic structures have been assigned depending on the Ln.[2−4] An examination of the electrical and magnetic properties of the various rare earth cobaltates, $Ln_{0.5}A_{0.5}CoO_3$ (A = alkaline earth), suggests that the properties are likely to be affected by both the average radius of the A-site cation and the cation disorder arising from size mismatch. Both the A-site cation radius and the size variance, $\sigma^2$, of the A-site cations are known to markedly affect the magnetic properties of the rare earth manganates of the general formula $Ln_{0.7}A_{0.3}MnO_3$.[6−8] Here, the variance, $\sigma^2$, is defined by

$$\sigma^2 = \sum x_i r_i^{\,2} - \langle r_A\rangle^2 \qquad (1)$$

where $x_i$ is the fractional occupancy of A-site ions, $r_i$ is the corresponding ionic radii and $\langle r_A\rangle$ is the weighted average radius calculated from the $r_i$ values. In the manganates, the size variance has a marked effect on the ferromagnetic properties of $Ln_{0.7}A_{0.3}MnO_3$, but appears to affect charge-ordering in $Ln_{0.5}A_{0.5}MnO_3$ only marginally.[9] In this article, we report the structures of several members of the $Ln_{0.5}A_{0.5}CoO_3$ family with A = Sr and Ba, based on Rietveld analysis of powder X-ray diffraction patterns. To understand the dependence of the ferromagnetic Curie temperature of $Ln_{0.5}A_{0.5}CoO_3$

---

* To whom correspondence should be addressed. E-mail: cnrrao@jncasr.ac.in.

(1) Jonker, G. H.; van Santen, J. H. *Physica* **1953**, *19*, 120. (b) Raccah, P. M.; Goodenough, J. B. *J. Appl. Phys.* **1968**, *39*, 1209. (c) Rao, C. N. R.; Prakash, O.; Bahadur, D.; Ganguly, P.; Nagabhushana, S. *J. Solid State Chem.* **1977**, *22*, 353. (d) Señarís-Rodríguez, M. A.; Goodenough, J. B. *J. Solid State Chem.* **1995**, *118*, 323.

(2) Moritomo, Y.; Takeo, M.; Liu, X. J.; Akimoto, T.; Nakamura, A. *Phys. Rev.* **1998**, *B58*, R13334.

(3) Troyanchuk, I. O.; Kasper, N. V.; Khalyavin, D. D.; Szymczak, H.; Szymczak. R. Baran, M. *Phys. Rev.* **1998**, *B58*, 2418.

(4) Troyanchuk, I. O.; Kasper, N. V.; Khalyavin, D. D.; Szymczak, H.; Szymczak. R. Baran, M. *Phys. Rev. Lett.* **1998**, *80*, 3380.

(5) Brinks, H. W.; Fjellvåg, H.; Kjekshus, A.; Hauback, B. C. *J. Solid State Chem.* **1999**, *147*, 464.

(6) Rodriguez-Martinez, L. M.; Attfield, J. P. *Phys. Rev.* **1996**, *B54*, R15622.

(7) Attfield, J. P. *Chem. Mater.* **1998**, *10*, 3239.

(8) Damay, F.; Martin, C.; Maignan, A.; Raveau, B. *J. Appl. Phys.* **1997**, *82*, 6181.

(9) Vanitha, P. V.; Santhosh, P. N.; Singh, R. S.; Rao, C. N. R.; Attfield, J. P. *Phys. Rev.* **1999**, *B59*, 13539.

10.1021/cm990268t CCC: $19.00

**Table 1. Structure and Properties of $Ln_{0.5}A_{0.5}CoO_3$**

| Ln | A | space group | $\langle r_A \rangle$ (Å) | $\sigma^2$ (Å$^2$) | lattice parameter (Å) | | | $T_C$ (K) |
|---|---|---|---|---|---|---|---|---|
| | | | | | *a* | *b* | *c* | |
| La | Sr | $R\bar{3}c$[a] | 1.400 | 0.0016 | 5.4152 | | | 258 |
| Nd | Sr | $R\bar{3}c$[b] | 1.355 | 0.0072 | 5.3770 | | | 226 |
| Gd | Sr | *Pnma* | 1.329 | 0.0123 | 5.3746 | 7.5601 | 5.3723 | 162 |
| La | Ba | $R\bar{3}c$[c] | 1.485 | 0.0156 | 5.4997 | | | 219 |
| Nd | Ba | *Pmmm* | 1.317 | 0.0240 | 11.7100 | 11.6778 | 7.6130 | 178 |
| Gd | Ba | *Pmmm* | 1.288 | 0.0330 | 11.7196 | 11.6323 | 7.5392 | |

[a] α = 60.17°. [b] α = 60.28°. [c] α = 60.04°.

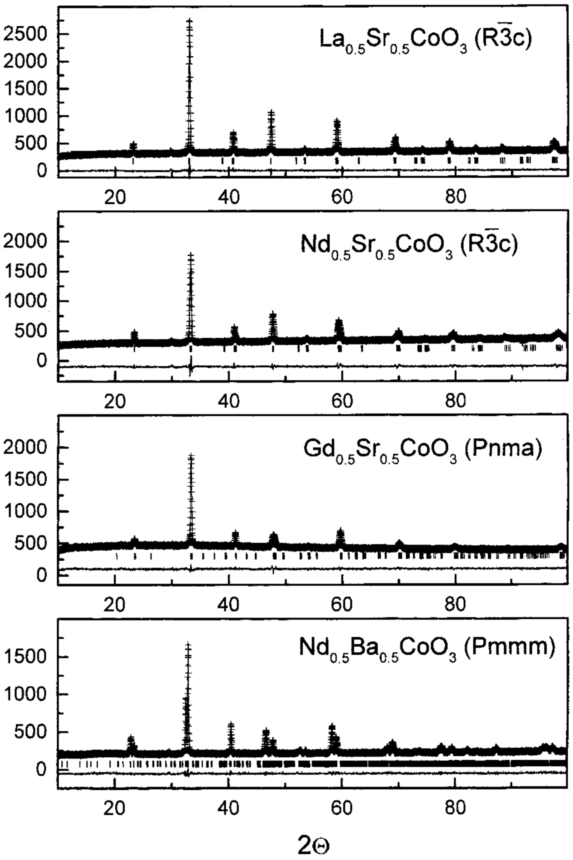

**Figure 1.** XRD patterns for the representative members of $Ln_{0.5}A_{0.5}CoO_3$. The calculated profile and the difference curve obtained from Rietveld analysis are also shown.

**Table 2. Atomic Coordinates of a Few Members of the $Ln_{0.5}A_{0.5}CoO_3$ Family**

| Ln | A | atom | site | *x* | *y* | *z* | $U_{iso}$ |
|---|---|---|---|---|---|---|---|
| La | Sr | La/Sr | 2a | 0.25000 | 0.25000 | 0.25000 | 0.00350 |
| | | Co | 2b | 0.00000 | 0.00000 | 0.00000 | 0.00376 |
| | | O | 6e | 0.28006 | 0.21994 | 0.75000 | 0.01221 |
| Nd | Sr | Nd/Sr | 2a | 0.25000 | 0.25000 | 0.25000 | 0.00611 |
| | | Co | 2b | 0.00000 | 0.00000 | 0.00000 | 0.00606 |
| | | O | 6e | 0.29662 | 0.20338 | 0.75000 | 0.00118 |
| Gd | Sr | Gd/Sr | 4c | 0.00407 | 0.25000 | 0.00490 | 0.02818 |
| | | Co | 4b | 0.00000 | 0.00000 | 0.50000 | 0.02018 |
| | | O | 8d | 0.30840 | −0.00712 | 0.25408 | 0.05097 |
| | | O | 4c | 0.08477 | 0.2500 | 0.50490 | −0.03259 |
| Nd | Ba | Nd/Ba | 1c | 0.00000 | 0.00000 | 0.50000 | 0.00959 |
| | | Nd/Ba | 2n | 0.00000 | 0.67102 | 0.50000 | 0.01407 |
| | | Nd/Ba | 2j | 0.31649 | 0.00000 | 0.50000 | 0.04112 |
| | | Nd/Ba | 4z | 0.33870 | 0.67146 | 0.50000 | 0.00225 |
| | | Nd/Ba | 1a | 0.00000 | 0.00000 | 0.00000 | −0.00658 |
| | | Nd/Ba | 2m | 0.00000 | 0.66496 | 0.00000 | −0.01020 |
| | | Nd/Ba | 2I | 0.33424 | 0.00000 | 0.00000 | −0.01217 |
| | | Nd/Ba | 4y | 0.32853 | 0.66496 | 0.00000 | 0.00080 |
| | | Co | 2t | 0.50000 | 0.50000 | 0.74589 | −0.04881 |
| | | Co | 4v | 0.50000 | 0.82006 | 0.73592 | 0.04939 |
| | | Co | 4x | 0.84936 | 0.50000 | 0.74713 | −0.00517 |
| | | Co | 8$\mu$ | 0.82403 | 0.16557 | 0.25343 | −0.00720 |
| | | O | 1h | 0.50000 | 0.50000 | 0.50000 | 0.13774 |
| | | O | 2p | 0.50000 | 0.84084 | 0.50000 | −0.03272 |
| | | O | 2l | 0.15382 | 0.50000 | 0.50000 | 0.06328 |
| | | O | 4z | 0.18089 | 0.84139 | 0.50000 | 0.09803 |
| | | O | 2s | 0.50000 | 0.00000 | 0.70000 | −0.00021 |
| | | O | 4v | 0.50000 | 0.66554 | 0.69596 | −0.07491 |
| | | O | 4w | 0.86807 | 0.00000 | 0.76102 | −0.02076 |
| | | O | 8$\mu$ | 0.83519 | 0.33170 | 0.27143 | −0.01216 |
| | | O | 2r | 0.00000 | 0.50000 | 0.71388 | −0.00142 |
| | | O | 4u | 0.00000 | 0.83147 | 0.69421 | 0.02978 |
| | | O | 4x | 0.66299 | 0.50000 | 0.73289 | 0.04036 |
| | | O | 8$\mu$ | 0.67560 | 0.16653 | 0.28503 | 0.03245 |
| | | O | 1f | 0.50000 | 0.50000 | 0.00000 | −0.04651 |
| | | O | 2o | 0.50000 | 0.81642 | 0.00000 | −0.07971 |
| | | O | 2k | 0.18571 | 0.50000 | 0.00000 | −0.04482 |
| | | O | 4y | 0.16576 | 0.85300 | 0.00000 | 0.07722 |

on $\langle r_A \rangle$ as well as cation disorder, we have examined the magnetic and electrical properties of several of these materials. In particular, we have investigated the variation of the properties of the cobaltates with constant $\langle r_A \rangle$, but variable $\sigma^2$.

## Experimental Section

Cobaltates of the general formula $Ln_{0.5}A_{0.5}CoO_3$ (Ln = rare earth, A = Sr or Ba) were prepared by the ceramic route. Stoichiometric quantities of the respective rare earth oxides, the carbonates of the alkaline earth elements, and cobalt oxide ($Co_3O_4$) were ground and prefired at 900 °C for 12 h in air. The powder so obtained was ground thoroughly and heated at 1000 °C for 12 h, and the pellets were finally sintered at 1200 °C. The samples were heated in oxygen atmosphere at a lower temperature to improve the oxygen stoichiometry. The phase purity of the samples was established by recording the X-ray diffraction patterns with a SEIFERT 3000 TT diffractometer. X-ray diffraction patterns of all the $Ln_{0.5}Sr_{0.5}CoO_3$ and $Ln_{0.5}Ba_{0.5}CoO_3$ compositions gave sharp reflections (fwhm $\approx$ 0.07°). Rietveld analysis of the powder X-ray diffraction data was carried out using the GSAS software suite.[10] The unit cell parameters of representative cobaltates are listed in Table 1. In Table 1, we have also listed the weighted average radius, $\langle r_A \rangle$, and the $\sigma^2$ values of these materials. The $\langle r_A \rangle$ values were calculated using the Shannon-radii, $r_i$, for 12-coordination in the case of the rhombohedral cobaltates and for 9-coordination in the case of orthorhombic ones. Two series of rhombohedral cobaltates of the general formula $Ln_{0.5-x}Ln'_xA_{0.5-y}A'_yCoO_3$ with constant $\langle r_A \rangle$ values of ~1.357 Å and 1.369 Å were prepared to study the effect of the A-site cation-size mismatch on the properties. These materials were prepared in the manner described earlier.

Electrical resistivity measurements were carried out from 300 to 20 K by the four-probe method. Magnetization measurements were carried out in the temperature range 300−80 K by means of a vibrating sample magnetometer (Lakeshore VSM 7300). The oxygen stoichiometry was determined by iodometric titrations. The error in oxygen content was ±0.02. The oxygen stoichiometry in the cobaltates studied by us was generally within this experimental error. Magnetoresistance measurements were carried out using a cryocooled closed cycle superconducting magnet.

## Results and Discussion

Rietveld analysis of the powder X-ray diffraction data of the cobaltates gave good fits as shown for four of the materials in Figure 1. The atomic coordinates for some of the cobaltates are given in Table 2. The structural

---

(10) Larson, A. C.; Von Dreele, R. B. *GSAS: General Structural Analysis System*; LANSCE, Los Alamos National Laboratory: Los Alamos, NM, 1994.

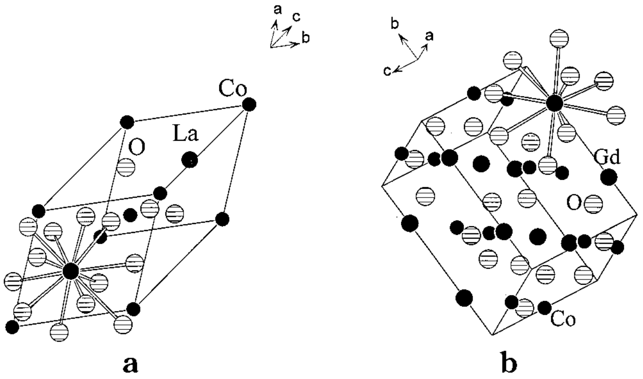

**Figure 2.** Rhombohedral and orthorhombic structures of representative members of $Ln_{0.5}A_{0.5}CoO_3$, showing different coordinations of the A-site cations: (a) La, Sr and (b) Gd, Sr.

**Table 3. Important Structural Parameters of a Few Members of $Ln_{0.5}A_{0.5}CoO_3$**

| $Ln_{0.5}A_{0.5}CoO_3$ | | bond distances | bond angles (deg) |
|---|---|---|---|
| Ln | A | (Å) Co−O | Co−O−Co |
| La | Sr | 6 × 1.9336 | 6 × 164.96 |
| Nd | Sr | 6 × 1.9217 | 6 × 164.94 |
| Gd | Sr | 2 × 1.7107 | 4 × 165.23 |
| | | 2 × 1.9444 | 2 × 152.85 |
| | | 2 × 2.1203 | |
| Nd | Ba[a] | 1 × 2.0989 | 2 × 180.00 |
| | | 1 × 2.0039 | 2 × 174.19 |
| | | 1 × 1.9488 | 2 × 159.31 |
| | | 1 × 1.9448 | |
| | | 1 × 1.8794 | |
| | | 1 × 1.7546 | |
| Gd | Ba[a] | 1 × 1.9013 | 1 × 174.72 |
| | | 1 × 1.8984 | 1 × 172.08 |
| | | 2 × 1.8932 | 1 × 169.15 |
| | | 1 × 1.8749 | 2 × 165.93 |
| | | 1 × 1.8724 | 1 × 151.58 |

[a] There are other unique sets of six Co−O distances in this compound, and we have only listed one representative set.

data reveal that when A = Sr, the structure is rhombohedral (space group: $R\bar{3}c$) up to Ln = Nd. In the case of $Nd_{0.5}Sr_{0.5}CoO_3$, we could get an equally good fit for the *Pnma* and $R\bar{3}c$ space groups, and we have, therefore, preferred the space group with higher symmetry as per the normal practice. When Ln = Gd, the structure is orthorhombic (space group: *Pnma*). The corresponding Ba compounds, except for La, are orthorhombic with the space group *Pmmm*. The A-site coordination number is 12 when the structure is rhombhohedral, and 9 when it is orthorhombic. In Figure 2, we show rhombohedral and orthorhombic structures for purpose of illustration. In Table 3 we list some of the structural parameters. The Co−O bond distances listed in the table show how the $CoO_6$ octahedra are distorted in the orthorhombic structure, especially in the *Pmmm* space group of the Ba compounds.

In Figure 3a, we show the temperature variation of the magnetization of a few compositions of $Ln_{0.5}A_{0.5}CoO_3$.The $T_C$ values obtained from the magnetization data are listed in Table 1. In Figure 4, $T_C$ values obtained by us are plotted against $\langle r_A \rangle$, along with some of the data from the literature. The $T_C$ increases up to a $\langle r_A \rangle$ value of 1.40 Å and decreases thereafter. The shape of the curve in Figure 4 is similar to the $T_C - \langle r_A \rangle$ plot for $Ln_{0.7}A_{0.3}MnO_3$.[11,12] The decrease in $T_C$ for $\langle r_A \rangle > 1.40$ Å is likely to arise from A-site cation disorder, just as in the case of the manganates.[6−8]

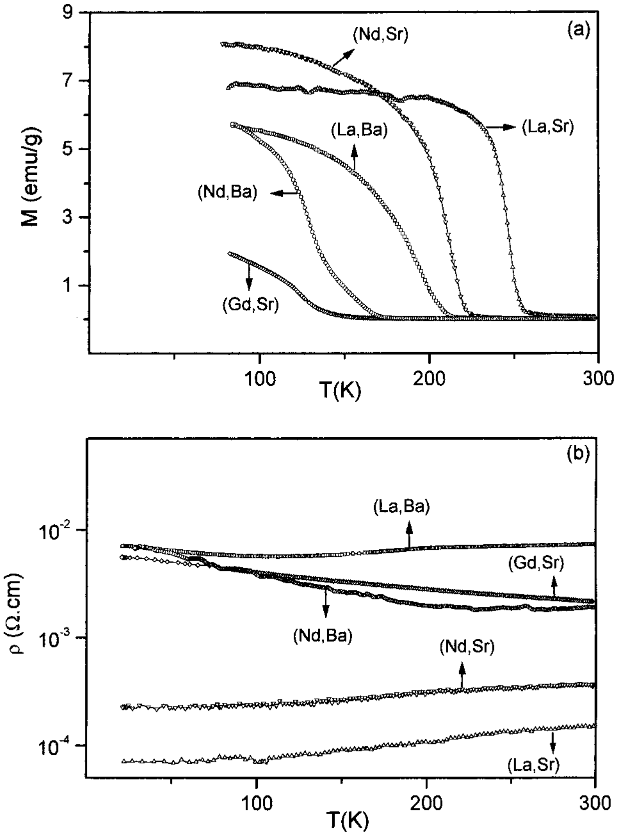

**Figure 3.** Temperature variation of (a) the magnetization, *M*, and (b) the electrical resistivity, *ρ*, of the cobaltates $Ln_{0.5}A_{0.5}CoO_3$. Ln and A are indicated in the figure.

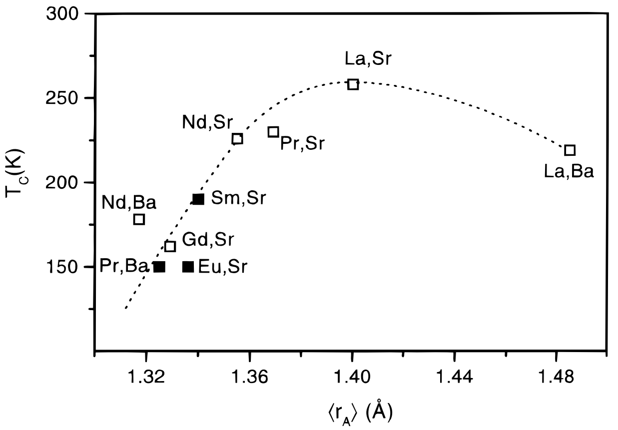

**Figure 4.** Variation of the ferromagnetic Curie temperature, $T_C$, with $\langle r_A \rangle$ in $Ln_{0.5}A_{0.5}CoO_3$. Ln and A are indicated in the figure. The filled symbols are the data from the literature. The broken curve is drawn as a guide to the eye.

Electrical resistivity data of the cobaltates also reflect the effect of cation size and disorder. In Figure 3b, we show the temperature variation of the electrical resistivity of the $Ln_{0.5}A_{0.5}CoO_3$ compounds. Both $La_{0.5}Sr_{0.5}CoO_3$ and $Nd_{0.5}Sr_{0.5}CoO_3$ show the expected metallic behavior, but orthorhombic $Gd_{0.5}Sr_{0.5}CoO_3$ shows a slight departure from metallic behavior. While $La_{0.5}Ba_{0.5}CoO_3$ is metallic, $Nd_{0.5}Ba_{0.5}CoO_3$ is an insulator. $Pr_{0.5}Ba_{0.5}CoO_3$ is reported to be an insulator.[3] It is

---

[11] Mahesh, R.; Mahendiran, R.; Raychaudhuri, A. K.; Rao, C. N. R. *J. Solid State Chem.* **1995**, *120*, 204.

[12] Hwang, H. Y.; Cheong, S. W.; Radaelli, P. G.; Marezio, M.; Batlogg, B. *Phys. Rev. Lett.* **1995**, *75*, 914.

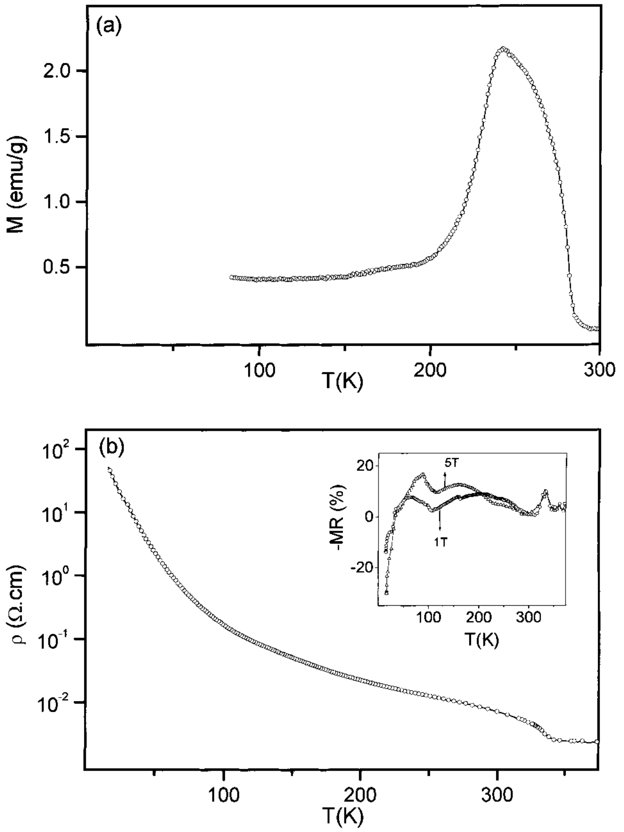

**Figure 5.** Temperature variation of (a) magnetization, *M*, and (b) resistivity, $\rho$, of the cobaltate, $Gd_{0.5}Ba_{0.5}CoO_3$. The inset in b shows the −MR (%) versus temperature plot in a field of 1 and 5 T.

**Table 4. Structure and Properties of $Ln_{0.5-x}Ln'_xA_{0.5-y}A'_yCoO_3$ with a Fixed $\langle r_A \rangle$ of 1.357 Å**

| | | lattice parameter | | |
|---|---|---|---|---|
| composition | $\sigma^2$ (Å$^2$) | $a$ (Å) | α (deg) | $T_C$ (K) |
| $Pr_{0.15}La_{0.35}Ca_{0.16}Sr_{0.34}CoO_3$ | 0.0026 | 5.3929 | 60.15 | 236 |
| $Nd_{0.15}La_{0.35}Sr_{0.355}Ca_{0.145}CoO_3$ | 0.0034 | 5.3913 | 60.23 | 233 |
| $Nd_{0.1}Pr_{0.4}Sr_{0.45}Ca_{0.05}CoO_3$ | 0.0053 | 5.3858 | 60.37 | 227 |
| $Gd_{0.11}Pr_{0.39}Sr_{0.5}CoO_3$ | 0.0070 | 5.3887 | 60.32 | 222 |
| $Nd_{0.5}Sr_{0.5}CoO_3$ | 0.0072 | 5.3770 | 60.28 | 226 |
| $Sm_{0.315}La_{0.185}Sr_{0.5}CoO_3$ | 0.0077 | 5.3883 | 60.24 | 223 |
| $Gd_{0.245}La_{0.255}Sr_{0.5}CoO_3$ | 0.0081 | 5.3948 | 60.16 | 217 |
| $Nd_{0.35}Gd_{0.15}Sr_{0.45}Ba_{0.05}CoO_3$ | 0.0118 | 5.3882 | 60.24 | 207 |
| $Sm_{0.5}Sr_{0.405}Ba_{0.095}CoO_3$ | 0.0157 | 5.3896 | 60.10 | 191 |
| $Nd_{0.2}Gd_{0.3}Sr_{0.395}Ba_{0.105}CoO_3$ | 0.0168 | 5.3943 | 60.01 | 181 |

**Table 5. Structure and Properties of $Ln_{0.5-x}Ln'_xA_{0.5-y}A'_yCoO_3$ with a Fixed $\langle r_A \rangle$ of 1.369 Å**

| | | lattice parameter | | |
|---|---|---|---|---|
| composition | $\sigma^2$ (Å$^2$) | $a$ (Å) | α (deg) | $T_C$ (K) |
| $Pr_{0.5}Sr_{0.5}CoO_3$ | 0.0051 | 5.3839 | 60.41 | 230 |
| $La_{0.235}Sm_{0.265}Sr_{0.5}CoO_3$ | 0.0070 | 5.3942 | 60.13 | 214 |
| $La_{0.315}Dy_{0.185}Sr_{0.5}CoO_3$ | 0.0085 | 5.3967 | 60.10 | 200 |
| $Pr_{0.3}Gd_{0.2}Sr_{0.41}Ba_{0.09}CoO_3$ | 0.0134 | 5.3982 | 60.08 | 176 |
| $Pr_{0.2}Gd_{0.3}Sr_{0.36}Ba_{0.14}CoO_3$ | 0.0178 | 5.4021 | 60.08 | 143 |

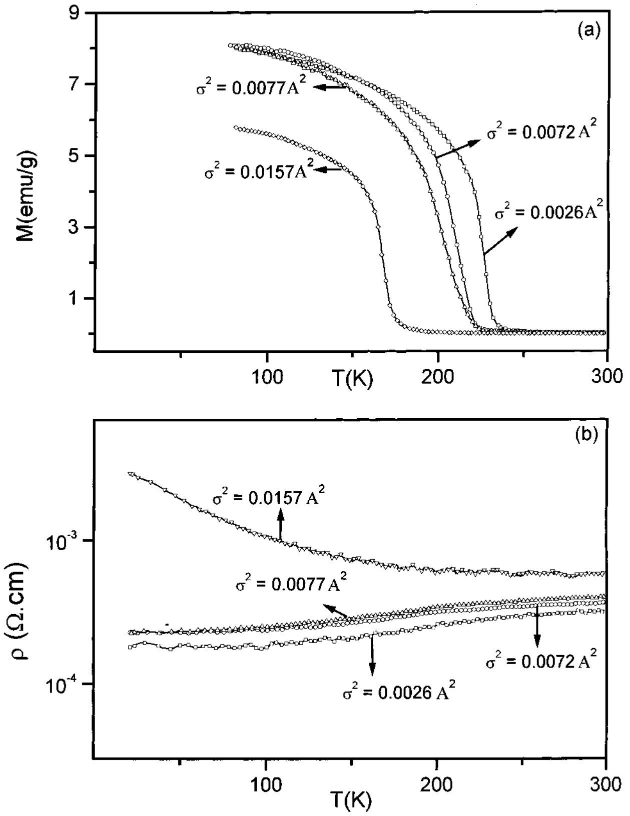

**Figure 6.** Temperature variation of (a) magnetization, *M*, and (b) resistivity, $\rho$, of rhombohedral $Ln_{0.5}A_{0.5}CoO_3$ with fixed $\langle r_A \rangle$ of 1.357 Å and variable $\sigma^2$. The $\sigma^2$ values are shown in the figure.

interesting that $Pr_{0.5}Ba_{0.5}CoO_3$ and $Nd_{0.5}Ba_{0.5}CoO_3$ are insulating, despite the large $\langle r_A \rangle$, unlike $La_{0.5}Ba_{0.5}CoO_3$ and the strontium analogues. This is likely due to the large cation-size disorder, with $\sigma^2 > 0.01$ Å$^2$. $Gd_{0.5}Sr_{0.5}CoO_3$ with $\sigma^2 \approx 0.012$ Å$^2$ tends to be insulating because it also has a relatively small $\langle r_A \rangle$. These results suggest that cation-size disorder can render a material insulating even though the $\langle r_A \rangle$ is considerably large, as in the case of $Ln_{0.5}Ba_{0.5}CoO_3$ (Ln = Pr, Nd). These results show the important role of cation size and disorder on both the magnetic and the electrical properties.

$Gd_{0.5}Ba_{0.5}CoO_3$ ($\langle r_A \rangle$ = 1.288 Å), with a large value of $\sigma^2$ (0.033 Å$^2$) as well as orthorhombic distortion, exhibits unique magnetic and transport properties. It is not ferromagnetic as the La, Pr, and Nd derivatives of the same series. Instead, it shows a metamagnetic type of transition around 240 K as illustrated in Figure 5a. A similar transition has been reported by Troyanchuk et al.[4] Across the magnetic transition, the material remains an insulator. $Gd_{0.5}Ba_{0.5}CoO_3$ also exhibits a small resistivity transition at 340 K as revealed in Figure 5b, in agreement with the reports in the literature.[2,4] This transition has been attributed to charge ordering of the $Co^{3+}$ and $Co^{4+}$ ions.[2] We do not however see the resistivity anomaly around 250 K reported by Troyanchuk et al.[4] Magnetoresistance measurements show about 17% negative magnetoresistance (MR) at 75 K in a field of 5 T, but no MR maximum at 250 K as reported by Troyanchuk et al.[4] There is a small increase in MR at 340 K where the resistivity transition occurs (Figure 5b).

To investigate the effect of the A-site cation-size mismatch on the magnetic and electrical properties of the cobaltates, we have systematically varied $\sigma^2$ in two series of compounds with fixed $\langle r_A \rangle$ values of 1.357 and 1.369 Å. We list the lattice parameters and $\sigma^2$ values in Tables 4 and 5. We show typical magnetization data of the series with $\langle r_A \rangle$ = 1.357 Å in Figure 6a to illustrate how the ferromagnetic $T_C$ decreases with the increase in $\sigma^2$. We have listed the $T_C$ values of the two series of cobaltates in Tables 4 and 5 and plotted the $T_C$ values

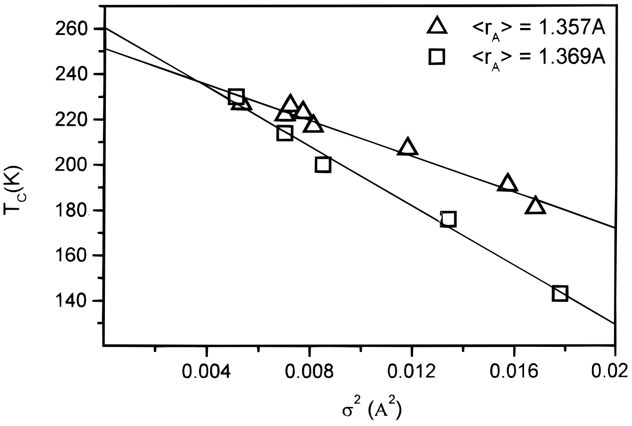

**Figure 7.** Variation of the ferromagnetic Curie temperature, $T_C$ with $\sigma^2$ in rhombohedral $Ln_{0.5}A_{0.5}CoO_3$ for fixed $\langle r_A \rangle$ values of 1.357 Å and 1.369 Å.

against $\sigma^2$ in Figure 7. The plots are fairly linear. We can write the relation as

$$T_C = T°_C - p\sigma^2 \qquad (2)$$

where the value of the intercept, $T°_C$ is an estimate of the ideal ferromagnetic Curie temperature that would have been observed in the absence of A-site cation-size disorder ($\sigma^2 = 0$). We find $T°_C$ to be 251 ± 3 K and 261 ± 4 K respectively for $\langle r_A \rangle$ values of 1.357 and 1.369 Å respectively, the corresponding slopes being 3961 ± 270 K $Å^{-2}$ and 6558 ± 369 K $Å^{-2}$. There is some variation in $T°_C$ in the cobaltates even for a change of 0.012 Å in $\langle r_A \rangle$, compared to the manganates where marked changes in $T°_C$ occur for larger changes in $\langle r_A \rangle$.[7,8] Furthermore, the slope of the $T_C - \sigma^2$ plot increases with $\langle r_A \rangle$ in the cobaltates while it decreases in the manganates.

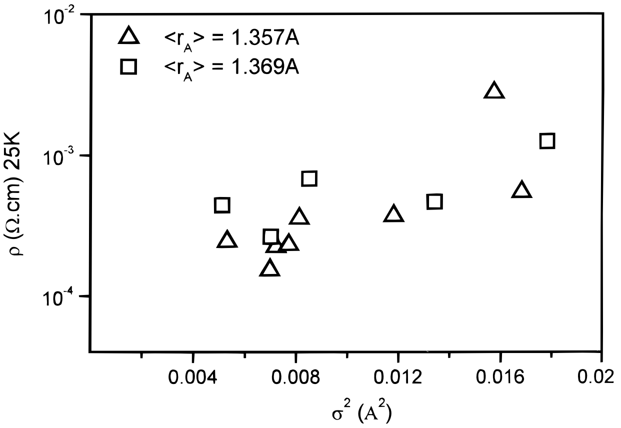

**Figure 8.** Variation of the resistivity of rhombohedral $Ln_{0.5}A_{0.5}$-$CoO_3$ at 25 K with $\sigma^2$.

In Figure 6b, we have plotted the electrical resistivity of the cobaltates in Table 4 with a fixed $\langle r_A \rangle$ of 1.357 Å. The materials are metallic for $\sigma^2 < 0.012$ $Å^2$ and become insulating at higher $\sigma^2$, as also corroborated by the data in Figure 3b. This metal–insulator transition is brought about entirely by size disorder. The rare earth cobaltates are distinct from the rare earth manganates in that the latter show an insulator–metal transition around the ferromagnetic $T_C$ and the transition temperature decreases with increase in $\sigma^2$. We have plotted the resistivity of $Ln_{0.5}A_{0.5}CoO_3$ at 25 K against $\sigma^2$ in Figure 8. We see a general increase in resistivity with increase in $\sigma^2$ in the cobaltates studied.

**Acknowledgment.** The authors thank Dr. A. R. Raju for assistance with the magnetoresistance measurements.

CM990268T